

Fig. 5 Effect of leading-edge roundness on the steady and unsteady longitudinal aerodynamics of a 69.6-deg delta wing (c.g. at 75% chord).

Figures 3–5 demonstrate that the experimentally observed,^{7–9} effects of wing thickness and leading-edge roundness on delta wing aerodynamics are well predicted. Inclusion of the effect of the cross-sectional geometry in the rapid prediction method developed earlier significantly improves the agreement with experiment. The high-alpha steady and unsteady aerodynamics of slender delta wing and wing-body configurations¹⁰ are predicted with sufficient accuracy for preliminary design, as long as vortex breakdown does not occur.

References

- ¹Polhamus, E. C., "Predictions of Vortex-Lift Characteristics by Leading-Edge Suction Analogy," *Journal of Aircraft*, Vol. 8, No. 4, 1971, pp. 193–199.
- ²Ericsson, L. E., and King, H. H. C., "Rapid Prediction of High-Alpha Unsteady Aerodynamics of Slender Wing Aircraft," *Journal of Aircraft*, Vol. 29, No. 1, 1992, pp. 85–82; see also AIAA Paper 90-3037, Aug. 1990.
- ³Jacobs, E. N., and Sherman, A., "Airfoil Section Characteristics as Affected by Variations in the Reynolds Number," NACA TR 586, 1937.
- ⁴Ericsson, L. E., and Reding, J. P., "Unsteady Aerodynamics of Slender Delta Wings at Large Angles of Attack," *Journal of Aircraft*, Vol. 12, No. 9, 1975, pp. 721–729; Errata, Vol. 14, Aug. 1977, p. 832.
- ⁵Wood, N. J., and Roberts, L., "Control of Vortical Lift on Delta Wings by Tangential Leading-Edge Blowing," *Journal of Aircraft*, Vol. 25, No. 3, 1988, pp. 236–243.
- ⁶Wood, N. J., and Roberts, L., "The Control of Delta Wing Aerodynamics at High Angles of Attack," Proceedings of the RAS Conference on the Prediction and Exploitation of Separated Flow, Paper 20, London, April 18–20, 1988.
- ⁷Peckham, D. H., "Low Speed Wind-Tunnel Tests on a Series of Uncambered, Slender, Pointed Wings with Sharp Leading Edges," Aeronautical Research Council, R&M 3186, Great Britain, Dec. 1958.
- ⁸Gersten, K., "Nichtlineare Tragflächen Theorie insbesondere für Tragflügel mit kleinen Seitenverhältnis," *Ingenieur-Archiv*, Vol. 30, 1961, pp. 431–452.
- ⁹Woodgate, L., "Measurements of the Oscillatory Pitching Moment Derivatives on a Delta Wing with Rounded Leading Edges in Incompressible Flow," Aeronautical Research Council, R&M 3628, Pt. 1, Great Britain, July 1968.
- ¹⁰Ericsson, L. E., and King, H. H. C., "Effect of Leading-Edge

Cross-Sectional Geometry on Slender Wing Unsteady Aerodynamics," AIAA Paper 92-0173, Jan. 1992.

Alternative Solution to Optimum Gliding Velocity in a Steady Head Wind or Tail Wind

Philip D. Bridges*

Mississippi State University,
Mississippi State, Mississippi 39762

Introduction

THE problem of graphically determining the velocity for the maximum gliding distance of an aircraft in a given atmosphere has been addressed by several authors.^{1–4} A comprehensive numerical analysis was performed by Jenkins and Wasyl⁵ in which they presented solutions for the optimum glide velocity and crab angle in a given wind and air mass sink rate. For the particular case of a direct head wind or tail wind and zero air mass sink rate, they found that the solution for the optimal velocity could be expressed as

$$V = (1/2a)[4a^2v^2 + 4a(c - bv)]^{1/2} - v \quad (1)$$

where V is the optimal glide velocity, v is the wind speed (tail wind is positive), and the coefficients a , b , and c are functions of wing loading, aspect ratio, the slope of the profile drag vs Reynolds number, and the best glide speed in zero-wind. This equation gives a mathematical solution to what has traditionally been shown by graphical analysis, that optimum glide velocity increases in a head wind and decreases in a tail wind.

An alternative solution to this particular problem can be found by assuming a parabolic drag polar for the glider and making small angle approximations to the glide angle. The optimum glide velocity is solved as an infinite power series involving only the wind speed and zero-wind optimum glide velocity, thus avoiding the requirement to find the coefficients in the previous equation.

Discussion

The analysis is begun by looking at an aircraft in a constant glide with velocity V and wind v (Fig. 1). The flight path angle of the glider with respect to the ground γ_g can be written as

$$\tan \gamma_g = (\dot{h}/V_g) \quad (2)$$

where \dot{h} is the sink rate and V_g is the velocity of the glider over the ground. By making the approximation that γ_g is small, the flight path angle can be expressed as

$$\gamma_g = [\dot{h}/(V + v)] \quad (3)$$

The sink rate can be eliminated by the relationship

$$\dot{h} = (C_L/C_D)V \quad (4)$$

with C_D and C_L the aircraft coefficients of drag and lift, respectively. The coefficient of drag can be expressed in the form of a parabolic drag equation, where the first term is the

Received Feb. 26, 1992; revision received Nov. 23, 1992; accepted for publication Nov. 30, 1992. Copyright © 1992 by the American Institute of Aeronautics and Astronautics, Inc. All rights reserved.

*Associate Professor, Department of Aerospace Engineering. Senior Member AIAA.

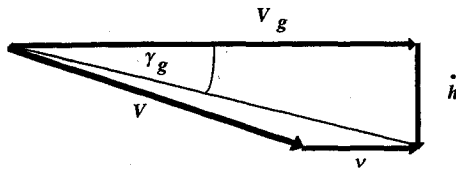


Fig. 1 Geometry of gliding flight.

constant zero-lift drag coefficient, and the second term is proportional to the square of the coefficient of lift,⁶ or

$$C_D = C_{D0} + KC_L^2 \quad (5)$$

Substituting Eqs. (4) and (5) into Eq. (3) gives the final form of the flight path angle as

$$\gamma_g = \frac{C_{D0} + KC_L^2}{C_L[1 + (v/V)]} \quad (6)$$

In order to maximize the range, it is necessary to minimize the flight path angle γ_g with respect to the aircraft velocity V . This is done by taking the derivative of Eq. (6) with respect to V , setting the resulting expression to zero, and solving for V . Taking this derivative and recognizing that C_L is also a function of V results in the fifth-order polynomial

$$\hat{V}^5 + \frac{3}{2}\hat{V}^4 - \hat{V} - (\hat{v}/2) = 0 \quad (7)$$

where the nondimensional velocities \hat{V} and \hat{v} are defined as

$$\hat{V} = (V/V_0) \quad \hat{v} = (v/V_0) \quad (8)$$

and are the ratios of the velocities to V_0 , the optimal glide velocity of the aircraft in zero-wind conditions. V_0 is found as a function of altitude and wing loading for each aircraft during initial certification and is thus a known quantity. The solution to Eq. (7) will yield the optimum glide velocity ratio \hat{V} in terms of the wind velocity ratio \hat{v} .

Solution

There is no general equation that will solve fifth-order or greater polynomials.⁷ This does not mean, however, that a solution does not exist. It just means that there is no easy way to find it. In order to try and get an idea for the solution, Eq. (7) was solved numerically using a Newton-Raphson iteration scheme. The results of this are shown in Fig. 2. As has been previously stated, the solution shows that a head wind requires a greater glide velocity, and a tail wind a lesser velocity. The points on the graph were then fitted with a least-squares curve fit, ranging sequentially from a second-order polynomial to a fourth-order polynomial. When this was done, an interesting phenomena occurred. Each successive curve-fit kept the previous terms and added an additional term of opposite sign. Thus, the three curve fits were

$$\hat{V} = 0.9968 - 0.3354\hat{v} + 0.2611\hat{v}^2 \quad (9)$$

$$\hat{V} = 0.9968 - 0.2547\hat{v} + 0.2611\hat{v}^2 - 0.1416\hat{v}^3 \quad (10)$$

$$\hat{V} = 0.9963 - 0.2547\hat{v} + 0.2235\hat{v}^2 - 0.1416\hat{v}^3 + 0.003255\hat{v}^4 \quad (11)$$

This pattern of adding an additional term of alternating sign and keeping the other terms essentially constant suggests that the solution to Eq. (7) consists of an infinite series of the form

$$\hat{V} = 1 + \hat{v} \sum_{n=0}^{\infty} a_n \hat{v}^n \quad (12)$$

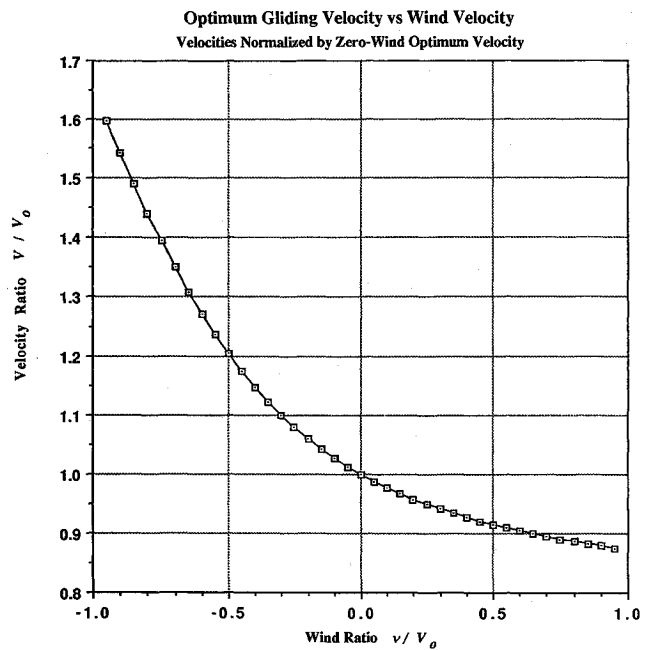


Fig. 2 Optimum velocity ratio.

with the limitation

$$-1 < \hat{v} < 1 \quad (13)$$

since Eq. (6) and its derivatives are not analytic at $\hat{v} = -1$. Substituting Eq. (12) into Eq. (7) and summing the like powers of \hat{v} to zero permits the sequential solution of the coefficients a_n , with the first five terms found to be

$$\begin{aligned} a_0 &= -\frac{1}{4} \\ a_1 &= \frac{7}{32} \\ a_2 &= -\frac{5}{32} \\ a_3 &= \frac{167}{2048} \\ a_4 &= -\frac{1}{64} \end{aligned} \quad (14)$$

The optimum glide velocity ratio can then be expressed as

$$\hat{V} = 1 - (\hat{v}/4)(1 - \frac{7}{8}\hat{v} + \frac{5}{8}\hat{v}^2 - \frac{167}{312}\hat{v}^3 + \frac{1}{16}\hat{v}^4 - \dots) \quad (15)$$

This closed-form solution shows clearly the effect of the wind on the optimum glide velocity ratio. For very small values of \hat{v} , the optimum velocity should be reduced by approximately $\frac{1}{4}$ of the tail wind or increased by $\frac{1}{4}$ of the head wind. The correction is not symmetrical, however, for larger values of \hat{v} . For negative values of \hat{v} (a head wind), all of the terms in the series are positive, with the result that the velocity correction for a head wind is larger than that for a tail wind.

A rule-of-thumb widely used in the glider community is to add $\frac{1}{2}$ of the wind speed to the zero-wind optimum glide velocity when gliding in a head wind.⁸ Equation (15) and Fig. 2, however, show that this rule gives too high an optimum velocity at head winds up to approximately $0.7V_0$, and too low a velocity at higher head wind speeds. The rule-of-thumb does not address tail winds, but the graph and equation indicate that the velocity correction as a percentage of the tail wind decreases with increasing tail wind. As the tail wind becomes infinitely large, the optimum airspeed will approach the minimum sinking speed of the glider. For a glider with a parabolic drag polar, this will result in an optimum velocity of $0.76V_0$.⁹

Jenkins et al.¹⁰ have shown that certain types of aircraft, even though physically different, have nearly identical optimum glide speeds over all geophysically realizable head winds

and tail winds. They argued that these differences could be explained by wing loading per aspect ratio and wing root thickness. The series solution shows that the optimum glide velocity in a head wind or tail wind depends only on the wind velocity and the zero-wind optimum glide velocity. Therefore, gliders with parabolic drag polars having identical zero-wind optimum glide velocities will have identical optimum velocities in a head wind or tail wind, despite having different geometric shapes and wing loading.

Conclusion

An alternative solution of the optimum gliding speed in a steady head wind or tail wind has been found. This equation solves the gliding velocity in terms of the zero-wind glide velocity and the wind velocity, and it clearly shows that the optimum glide velocity is solely determined by these two variables. The solution is valid for wind speeds up to the zero-wind optimum glide velocity and requires no curve fitting or coefficient calculations. The solution also demonstrates mathematically why a head wind will always require a greater velocity correction than a tail wind for optimum gliding flight.

Acknowledgments

The author would like to thank the reviewer for the helpful comments and criticisms that resulted in defining the region of convergence for the series solution. Acknowledgment is also given to the readers of the bulletin board "rec.aviation" who asked the question about optimum glide speed in a head wind or tail wind.

References

- ¹MacCready, P. B., "Optimum Airspeed Selector," *Soaring*, Vol. 18, No. 2, 1954, pp. 16-21.
- ²MacCready, P. B., "Understanding Speed-to-Fly and the Speed Ring," *Soaring*, Vol. 47, No. 5, 1982, pp. 42-47.
- ³Kuettner, J. P., "The 2000 Kilometer Wave Flight—Part II," *Soaring*, Vol. 49, No. 3, 1985, pp. 22-27.
- ⁴Reichmann, H., *Cross-Country Soaring*, Thomson, Pacific Palisades, CA, 1978, p. 98.
- ⁵Jenkins, S. A., and Wasyl, J., "Optimization of Glides for Constant Wind Fields and Course Headings," *Journal of Aircraft*, Vol. 27, No. 7, pp. 632-638.
- ⁶Shevell, R. S., *Fundamentals of Flight*, 2nd ed., Prentice-Hall, Englewood Cliffs, NJ, p. 185.
- ⁷Burrington, R. S., *Handbook of Mathematical Tables and Formulas*, 4th ed., McGraw-Hill, New York, p. 13.
- ⁸Soaring Society of America, *Soaring Flight Manual*, Jeppesen Sanderson, Inc., Englewood, CO, 1980, Chap. 2, p. 7.
- ⁹Miele, A., *Flight Mechanics—Theory of Flight Paths*, Vol. 1, Addison-Wesley, Reading, MA, 1962, p. 153.
- ¹⁰Jenkins, S. A., Armi, L., and Wasyl, J., "Glide Optimization for Cross Country Wave Flights," *Technical Soaring*, Vol. 16, No. 1, 1992, pp. 3-16.

Navier-Stokes Investigation of Blunt Trailing-Edge Airfoils Using O Grids

M. Khalid* and D. J. Jones†
Institute for Aerospace Research,
National Research Council of Canada,
Ottawa, Ontario K1A 0R6, Canada

Received June 25, 1992; revision received Nov. 2, 1992; accepted for publication Nov. 13, 1992. Copyright © 1992 by the American Institute of Aeronautics and Astronautics, Inc. All rights reserved.

*Associate Research Officer, High Speed Aerodynamics Laboratory.

†Senior Research Officer, High Speed Aerodynamics Laboratory. Member AIAA.

Introduction

SOME recent papers¹⁻³ have investigated the flowfield past a blunt trailing-edge airfoil. We show here that the standard ARC2D⁴ code (Baldwin-Lomax) can be used for blunt trailing-edge airfoils with the computational domain configured as an O-grid, rather than using a complex C-H-grid,¹ requiring higher order turbulence models for convergence. See Ref. 5 for details.

Four airfoils 1) RAE2822 (1.12%), 2) FIN5LLT1 (0.7%), 3) FINLLT2 (1.49%), and 4) WTEA (0.5%) were investigated. The percentages in brackets refer to the trailing-edge thickness with respect to the chord. The O-grids around the airfoils were generated using an algebraic generator ALGGRID.⁵ A typical O-grid around a blunt trailing-edge airfoil is shown in Fig. 1.

Results and Discussion

Figures 2 and 3 show the pressure coefficient comparisons with measured data for cases 1 and 2 for the RAE2822 airfoil. The agreement between the measured data (taken directly from Ref. 1) and computations for case 2 is quite good. For case 1, except for a small portion close to the leading edge on the upper surface, the pressures are well matched. The agreement for the lower surface, however, is not as good, especially in the forward regions.

The comparison of the coefficient of pressure with measured data, in the range $0.86 < x/c < 1.0$, for cases 1 and 2 are shown in Figs. 4 and 5, respectively. In this particular exercise the Navier-Stokes code was run with both the Baldwin-Lomax model as well as a mixing length turbulence model. The other results shown in the figures (taken from Ref. 1),

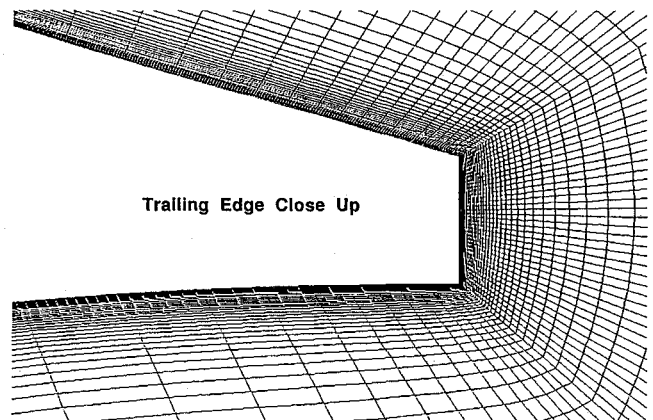


Fig. 1 Structured "O" grid around the blunt trailing-edge airfoil FIN5LLT2.

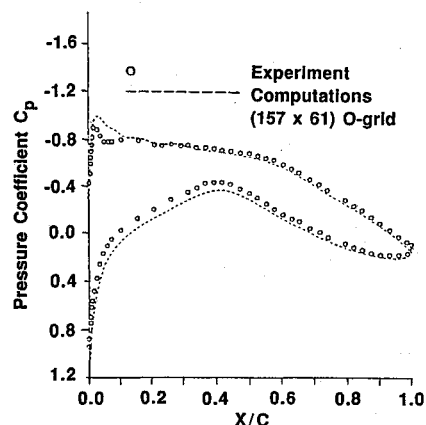


Fig. 2 Comparison of computed and measured data on blunt RAE2822 airfoil for case 1, $M_\infty = 0.676$, $\alpha = 2.45^\circ$, $Re = 5.4 \times 10^6$. Transition at $x/c = 0.11$ for upper and lower surfaces.